Cell Reports, Volume *27*

Supplemental Information

Partial Cone Loss Triggers Synapse-Specific Remodeling and Spatial Receptive Field Rearrangements in a Mature Retinal Circuit

Rachel A. Care, David B. Kastner, Irina De la Huerta, Simon Pan, Atrey Khoche, Luca Della Santina, Clare Gamlin, Chad Santo Tomas, Jenita Ngo, Allen Chen, Yien-Ming Kuo, Yvonne Ou, and Felice A. Dunn

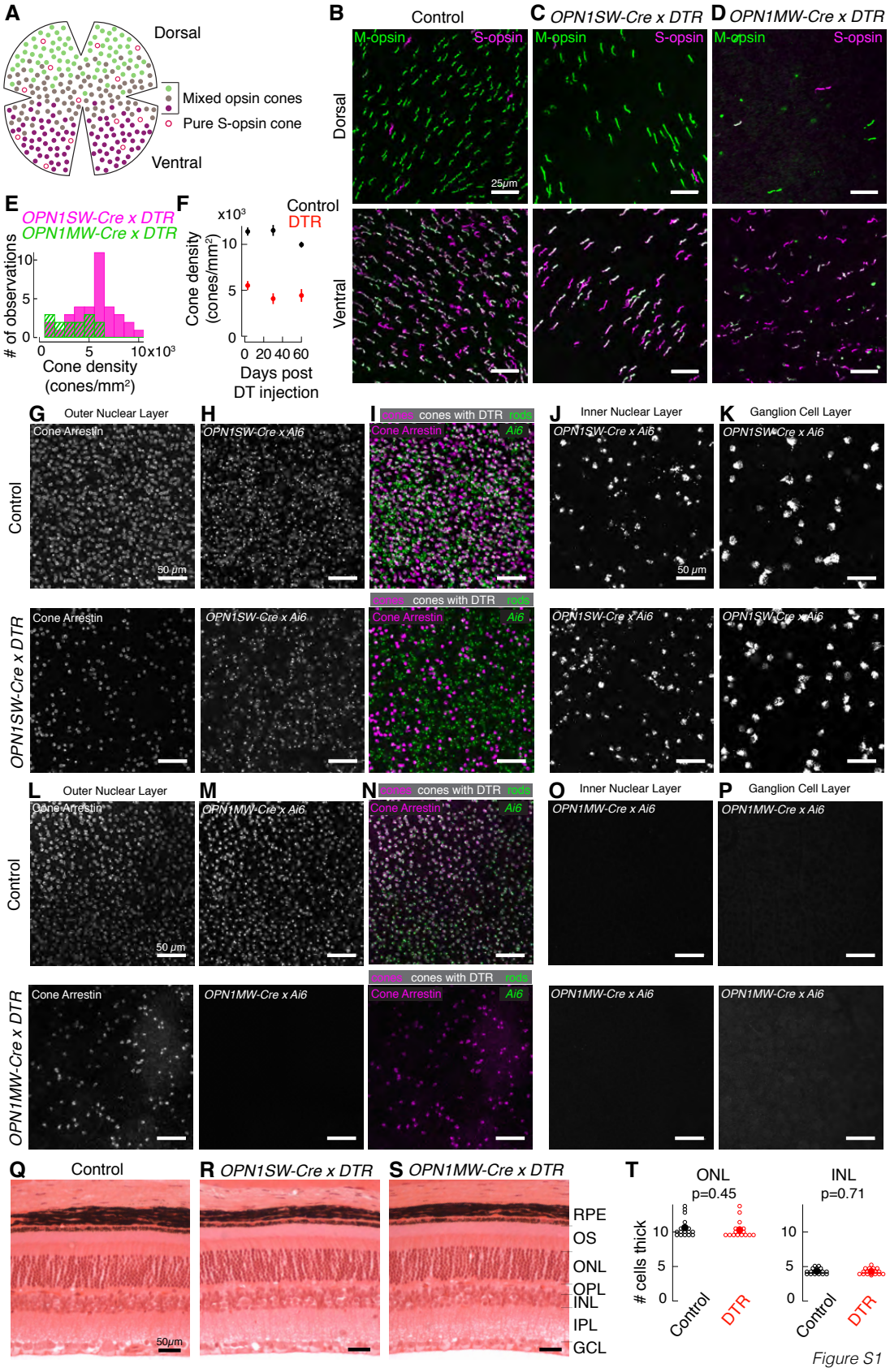
A
Dorsal
Mixed opsin cones
Pure S-opsin cone
Ventral
B Control
C OPN1SW-Cre x DTR
D OPN1MW-Cre x DTR
M-opsin
S-opsin
Dorsal
Ventral
25μm
E
OPN1SW-Cre x DTR
OPN1MW-Cre x DTR
# of observations
Cone density (cones/mm²)
F
Control
DTR
Cone density (cones/mm²)
Days post DT injection
G Outer Nuclear Layer
H
I cones with DTR rods
J Inner Nuclear Layer
K Ganglion Cell Layer
Control
OPN1SW-Cre x DTR
Cone Arrestin
OPN1SW-Cre x Ai6
Ai6
50 μm
L Outer Nuclear Layer
M
N cones with DTR rods
O Inner Nuclear Layer
P Ganglion Cell Layer
OPN1MW-Cre x DTR
OPN1MW-Cre x Ai6
Q Control
R OPN1SW-Cre x DTR
S OPN1MW-Cre x DTR
50μm
RPE
OS
ONL
OPL
INL
IPL
GCL
T
ONL
p=0.45
INL
p=0.71
# cells thick
Control
DTR

Figure S1

Figure S1. Diphtheria toxin system does not significantly affect other retinal cell types. Related to Figure 1.

(A) Schematic of the cone opsin distribution in mice in which middle wavelength (M) opsin is rich in dorsal retina (green), short wavelength (S) opsin is rich in ventral retina (magenta), and mixed opsin cones are found throughout retina.

(B-D) Confocal images of cone outer segments labeled in dorsal (top) and ventral (bottom) regions by the M opsin antibody (green) and S opsin antibody (magenta) in (B) control, (C) *OPN1SW-Cre x DTR*, and (D) *OPN1MW-Cre x DTR* retina. Both DTR lines spare cones with M and S opsin as shown by the persistence of cones containing M and S opsins.

(E) Histogram of cone density in *OPN1SW-Cre x DTR* (magenta) and *OPN1MW-Cre x DTR* (green) retina after DT injection. *OPN1SW* n = 35 retinas; *OPN1MW* n = 14 retinas.

(F) Cone density in control and DTR retina as a function of time since DT injection. One-way ANOVA was used to test for differences in cone density across intervals: Control $F(2, 31)=2.57$, $p=0.09$; DTR $F(2, 31)=1.2$, $p=0.32$.

(G-K) Confocal images of cell somas in the indicated layer from the *OPN1SW-Cre x Ai6* mouse line. (G) Cone somas labeled by cone arrestin in the outer nuclear layer. (H) Cone and rod somas that express Ai6 fluorescence. (I) Overlay of cone arrestin (magenta) and Ai6 fluorescence (green). Cones labeled with cone arrestin and not expressing Ai6 are magenta, cones labeled with cone arrestin and expressing Ai6 are white, and rods expressing Ai6 are green. Cones expressing Ai6 (white) are numerous in control retina (top row) and diminish in DTR retina (bottom row) after DT administration, while photoreceptors not expressing Ai6 (cones = magenta; rods = green) are unaffected by DT administration.

(J,K) Maximum intensity projections of the (J) inner nuclear layer and (K) ganglion cell layer show that Ai6 fluorescence in bipolar and amacrine cells (J) and displaced amacrine cells and ganglion cells (K) does not decrease after DT administration, indicating that these cell populations survive our dosage of DT.

(L-P) Confocal images of cell somas in the indicated layer from the *OPN1MW-Cre x Ai6* mouse line. (L) Cone somas labeled by cone arrestin in the outer nuclear layer. Cones remain in DTR retina (bottom row). (M) Cone somas that express Ai6 fluorescence. (N) Overlay of cone arrestin (magenta) and Ai6 fluorescence (green). Most cones express Ai6 (white, top), and no rods express Ai6 (absence of green). Cones expressing Ai6 (white) are numerous in control retina (top row) and completely killed in DTR retina (bottom row).

(O,P) Maximum intensity projections of the (O) inner nuclear layer and (P) ganglion cell layer show no Ai6 fluorescence in bipolar and amacrine cells (O) nor in displaced amacrine cells and ganglion cells (P). Retinal location was determined by Syt2 and SMI-32 staining.

(Q-S) Plastic sections from (Q) control, (R) *OPN1SW x DTR*, (S) *OPN1MW-Cre x DTR* retina. Sections stained with Hematoxylin and Eosin. Layers of the retina are labeled on the right: RPE = retinal pigment epithelium, OS = outer segments, ONL = outer nuclear layer containing 97% rod cell bodies and 3% cone cell bodies (Jeon et al., 1998), OPL = outer plexiform layer, INL = inner nuclear layer containing bipolar cell and amacrine cell bodies, IPL = inner plexiform layer, and GCL = ganglion cell layer.

(T) Quantification of number of cell bodies in each column of the OPL and INL in retinal sections cut close to the optic nerve head. Quantification taken at multiple locations within and across retinal sections. No significant difference in the number of photoreceptor cell bodies in

ONL nor in the number of bipolar and amacrine cell bodies in the INL between control and DTR retinas (rank sum).

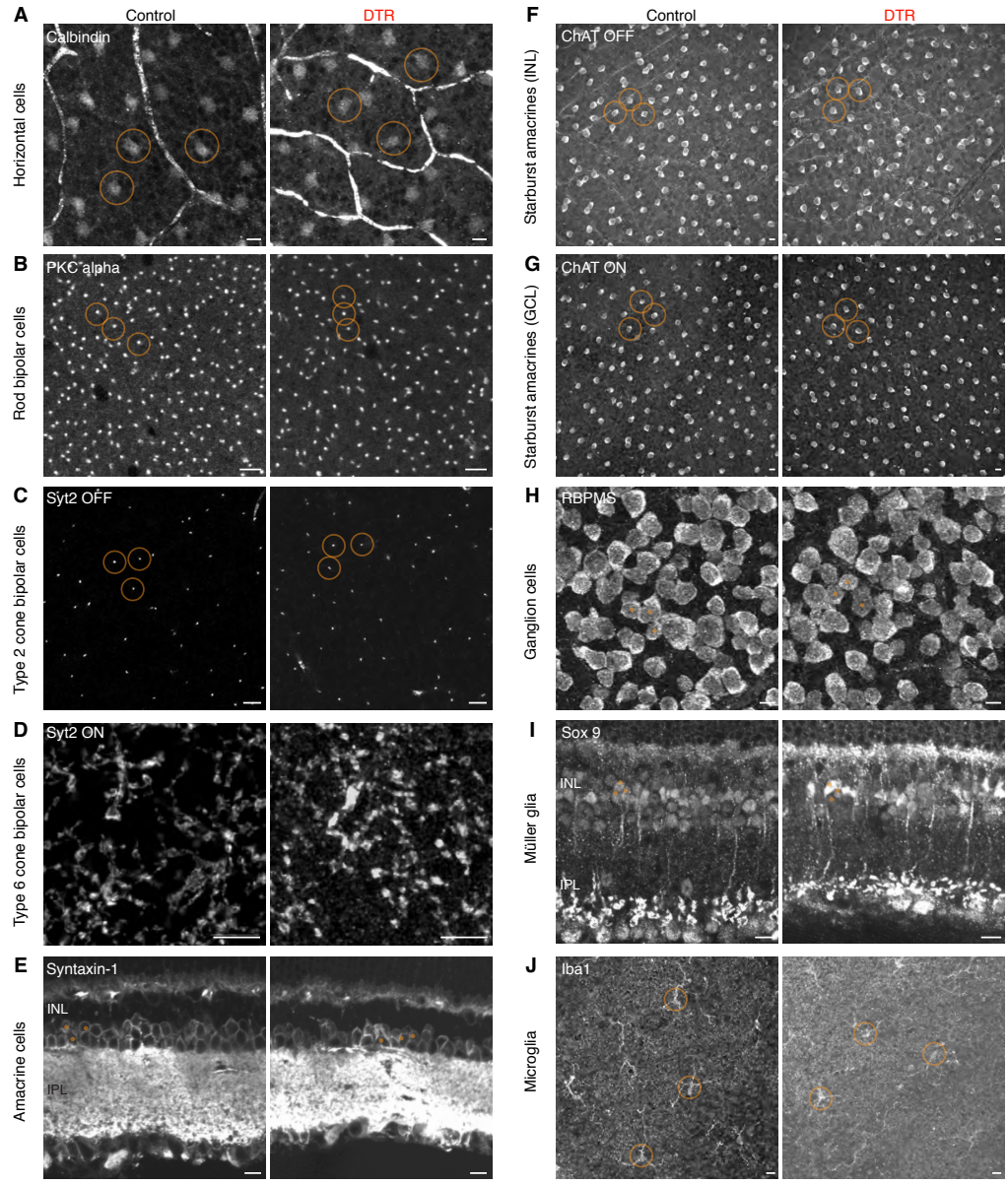

Figure S2

Figure S2. Effects of the diphtheria toxin system on non-cone retinal cell types. Related to Figure 1.

Example images of cell types under control and DTR conditions. When labeling was quantified, images show 3 examples of counts either by orange circles or dots. Quantification was done on areas larger than shown images (Table S1). (A) Horizontal cell somas labeled by calbindin in flat mount. (B) Rod bipolar cell axons stalks labeled by PKC alpha in flat mount. (C) Type 2 OFF cone bipolar cell axon stalks labeled by Syt2 in flat mount. (D) Type 6 ON cone bipolar cell axons labeled by Syt2 in flat mount. Syt2 labeling was variable between retinas and did not label the axon stalk and hence was not quantified. (E) Amacrine cell somas labeled by syntaxin-1 in sections. (F) Starburst amacrine cell somas in the inner nuclear layer (INL) labeled

by ChAT in flat mount. (G) Starburst amacrine cell somas in the ganglion cell layer (GCL) labeled by ChAT in flat mount. (H) Ganglion cell somas labeled by RBPMS in flat mount. (I) Müller glia labeled by Sox 9 in the section. (J) Microglia labeled by Iba1 at the level of the outer plexiform layer in flat mount. All scale bars = 10μm.

Cell Type	Methods: antibody, retinal layer imaged, flat mount or section, retinal topography if specific	Control Density (median±IQR)	DTR Density (median ±IQR)	n = images for control (& DTR) N = mice for control (& DTR)	Rank sum test p-value
Horizontal cells	Calbindin, ONL, flat mount, dorsal-nasal	1011.7±372.7 cells/mm^2	842.0±83.2 cells/mm^2	n = 6 (4) N = 3 (2)	p = 0.17
Rod bipolar cells	PKCalpha, IPL, flat mount, dorsal-nasal	16474±2127 cells/mm^2	15146±945 cells/mm^2	n = 8 (6) N = 3 (3)	p = 0.23
Type 2 OFF cone bipolar cells	Syt2, IPL, flat mount, dorsal-nasal	2983.6±189.8 cells/mm^2	2630.6±279.7 cells/mm^2	n = 4 (6) N = 2 (3)	p = 0.019
Amacrine cells	Syntaxin-1, INL, sections	280.0±59.8 cells/mm	278.8±54.0 cells/mm	n = 4 (4) N = 2 (2)	p = 0.69
Starburst amacrine cells (OFF)	ChAT, INL, flat mount, dorsal-nasal	1202.1±163.2 cells/mm^2	1168.8±326.3 cells/mm^2	n = 4 (6) N = 2 (3)	p = 0.50
Starburst amacrine cells (ON)	ChAT, GCL, flat mount, dorsal-nasal	1142.1±183.1 cells/mm^2	1092.2±166.5 cells/mm^2	n = 4 (6) N = 2 (3)	p = 0.50
Ganglion cells	RBPMS, GCL, flat mount, dorsal-nasal	3346.5±978.0 cells/mm^2	2967.3±1403.8 cells/mm^2	n = 7 (6) N = 3 (3)	p = 0.73
Müller glia	Sox9, INL, sections	414.2±62.7 cells/mm	246.5±164.0 cells/mm	n = 4 (4) N = 2 (2)	p = 0.06
Microglia	Iba1, OPL, flat mount, dorsal-nasal	103.2±23.2 cells/mm^2	109.9±10.0 cells/mm^2	n = 4 (4) N = 2 (2)	p = 0.83

Table S1. Effects of the diphtheria toxin system on the densities of non-cone retinal cellstypes. Related to Figure 1.

Quantification of major cell types in the retina under control and DTR conditions. Number of cell bodies was either quantified in flat mount (area density) or sections (linear density). Only the type 2 OFF cone bipolar cells show a significant decrease in density. Retinal layers: OPL = outer plexiform layer, ONL = outer nuclear layer, INL = inner nuclear layer, IPL = inner plexiform layer, and GCL = ganglion cell layer.

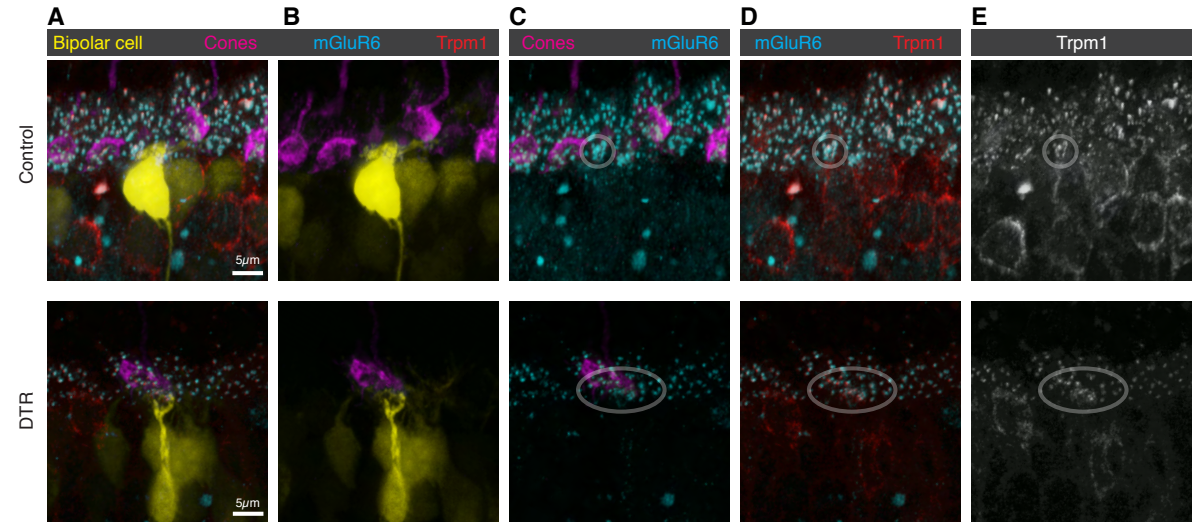

Figure S3

Figure S3. Transduction channel Trpm1 colocalizes with mGluR6. Related to Figure 3.
(A) Sections of (top) control and (bottom) DTR retina. Confocal images of a type 6 cone bipolar cell labeled by *Grm6-TdTomato* (yellow), cones labeled by cone arrestin (magenta), glutamate receptor labeled by mGluR6 (cyan), and transduction channel labeled by Trpm1 (red).
(B) Bipolar cell dendrites contacting nearby cones. In the DTR retina, only a single cone remains in the vicinity.
(C) mGluR6 is clustered at the pedicles of cones (ovals), whereas rod-associated mGluR6 is punctate.
(D) mGluR6 and Trpm1 colocalize both at the cone-associated clusters (ovals) and at the rod-associated puncta. (Bottom) In the absence of other cones, we find no evidence for clusters of cone-associated mGluR6 or Trpm1 by itself, suggesting that both proteins are either present or absent.
(E) Trpm1 colocalizes at cone-associated clusters, rod-associated puncta, and around the somas of ON bipolar cells.

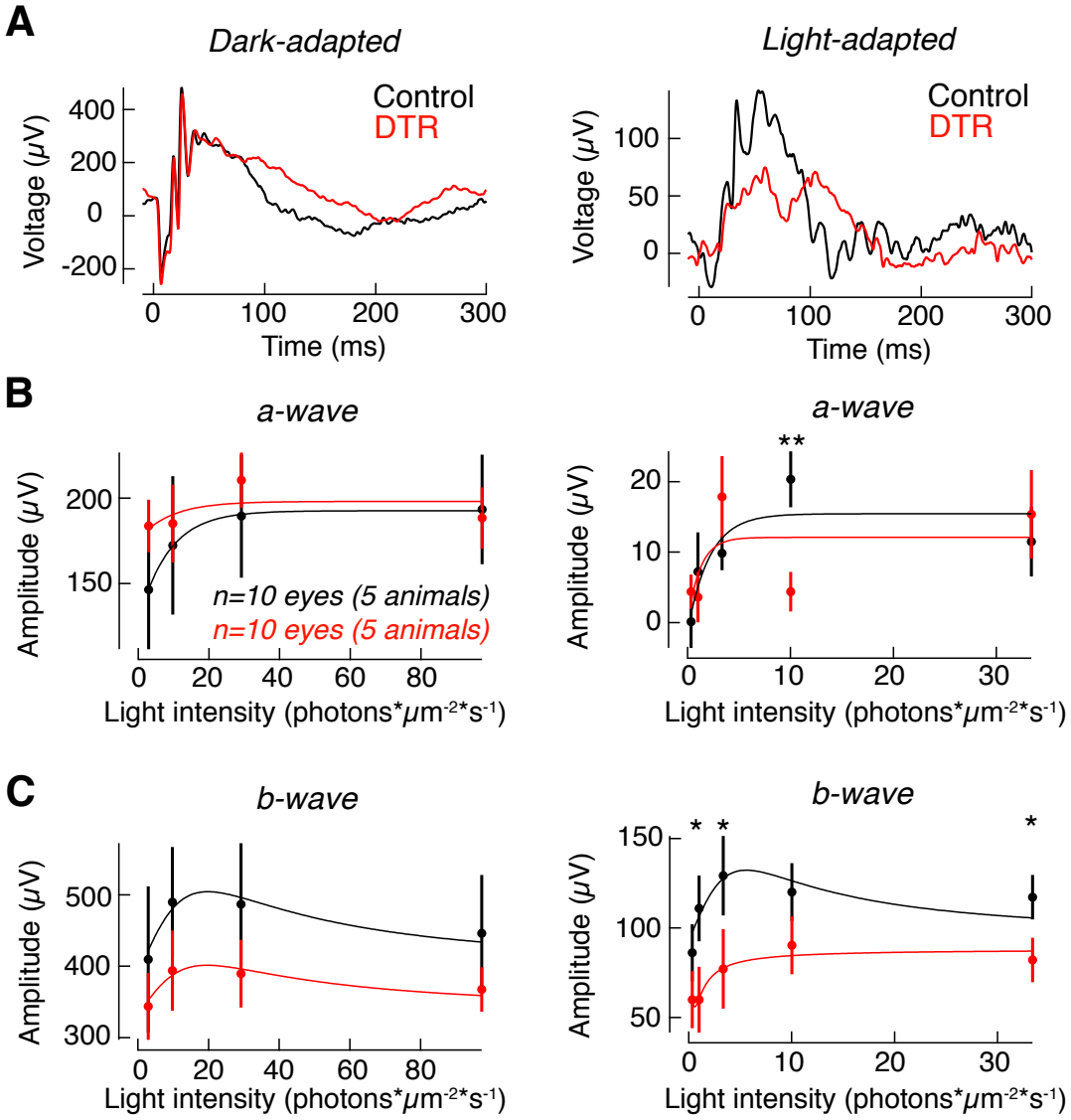

Figure S4

Figure S4. The photopic, but not scotopic, electroretinogram response is decreased after partial cone ablation. Related to Figure 4.

(A) Example traces of ERGs from control (black) and DTR (red) mice show an intact response at scotopic light levels (left) and a diminished response at photopic light levels (right). Traces shown are averages of recordings from the right and left eyes, which were made simultaneously.

(B) Absolute value of the a-wave amplitude, a measure of photoreceptor activity, across a range of light levels is maintained at scotopic light levels (left) but reduced in photopic light levels (right). Data fit with a single exponential function. (In light-adapted condition at 10.02

photons*μm^{-2}*s^{-1}: Control: 20.36±4.0μV, n=10 eyes from 5 animals; DTR: 4.39±2.8μV, n=10 eyes from 5 animals; mean±sem; p=0.0077, t-test).
(C) Amplitude of the b-wave, a measure of ON bipolar cell activity, across a range of light levels is maintained at scotopic light levels (left) but reduced in photopic light levels (right). Data fit with a serpentine function. (In light-adapted condition: at 1.00 photons*μm^{-2}*s^{-1}: Control: 110.94±18.4μV; DTR: 59.98±11.1μV; p=0.0332; at 3.34 photons*μm^{-2}*s^{-1}: Control: 129.19±22.3μV; DTR: 77.14±6.9μV; p=0.0387; at 33.4 photons/μm^{2}*s^{-1}: Control: 117.27±12.43μV; DTR: 82.19±9.5μV; p=0.0431; n=10 eyes from 5 animals; mean±sem; t-test).

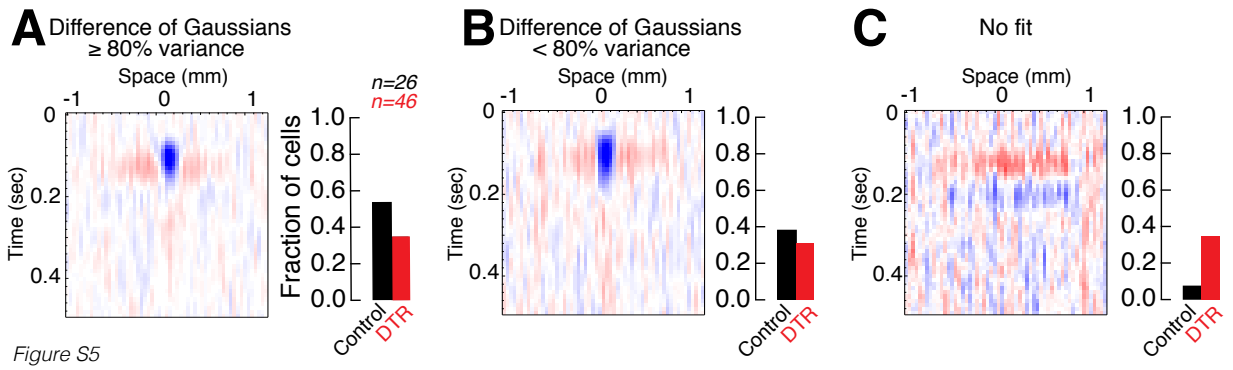

Figure S5

Figure S5. $A_{ON\text{-}S}$ ganglion cell from DTR retina exhibit a range of receptive field structures. Related to Figure 5.

(A) Spatio-temporal receptive field for a cell from DTR retina which was fit by a difference of Gaussians and for which ≥80% of the response variance in time was described by the first principal component. Bar graph (right) indicates that 53.8% of control and 34.8% of DTR cells fell into this category. Total number of ganglion cells in control and DTR retina indicated by n.

(B) Spatio-temporal receptive field for a cell from DTR retina which was fit by a difference of Gaussians and for which <80% of the response variance in time was described by the first principal component. Bar graph (right) indicates that 38.5% of control and 30.4% of DTR cells fell into this category.

(C) Spatio-temporal receptive field for a cell from DTR retina which was not fit by a difference of Gaussians. Bar graph (right) indicates that 7.7% of control and 34.8% of DTR cells fell into this category. These cells were not included in the receptive field analysis in Figure 5.